



Observation Characteristics of Airborne GNSS Radio Occultation in Atmospheric Rivers: Accuracy, Resolution, and Pathway to Near-real-time Operation

Bing Cao¹, Jennifer S. Haase¹, Noah Barton¹, Kate Lord¹, Anna M. Wilson², Michael J. Murphy^{1,3}

1. Institute of Geophysics and Planetary Physics, Scripps Institution of Oceanography, University of California San Diego
 2. Center for Western Weather and Water Extremes (CW3E), SIO, UCSD
 3. Now at NASA GMAO

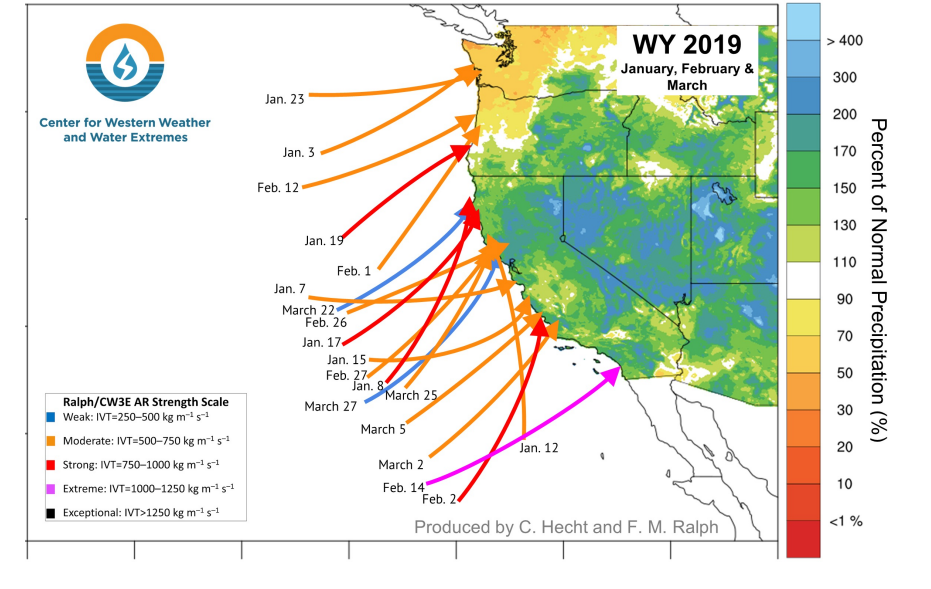
bic020@ucsd.edu Bing Cao,
 jhaase@ucsd.edu Jennifer Haase



1. Science Objectives

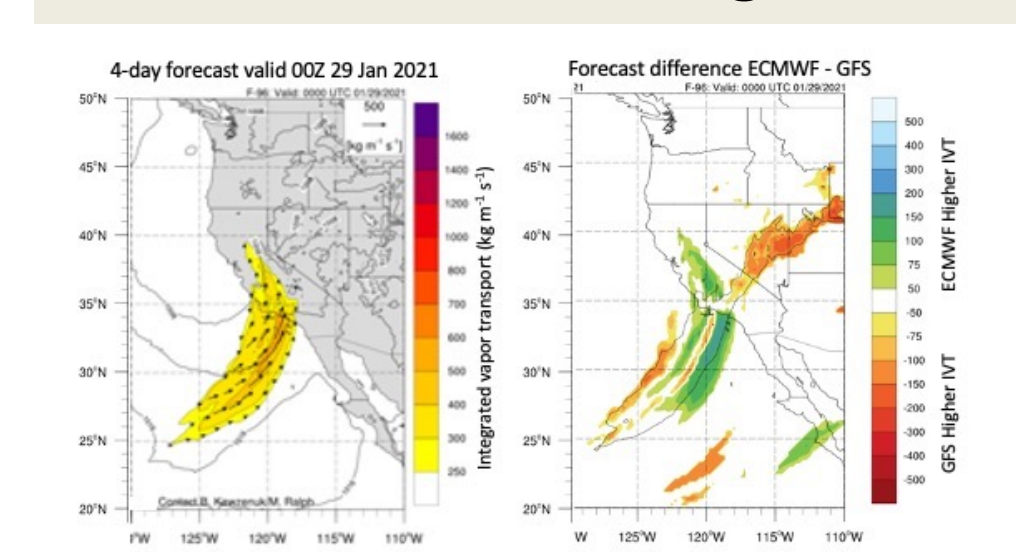
ARs alleviate drought and cause flooding.

- Atmospheric Rivers (ARs) transport water vapor between the tropics and mid-latitudes.
- 84 % of all flooding damages over 40 years in the western US are from ARs. They also contribute to the water supply and alleviate droughts.
- Forecast errors exist in the ARs' landfalling locations (several hundred km) and intensities, which have a significant impact on snowpack and watersheds.
- Direct measurements taken from reconnaissance aircraft that densely sample the target areas at desired times have an advantage for synoptic-scale to mesoscale systems such as ARs and tropical cyclones.
- AR reconnaissance campaign (AR Recon) supports AR forecasting for flood management and reservoir operations for water resources management.



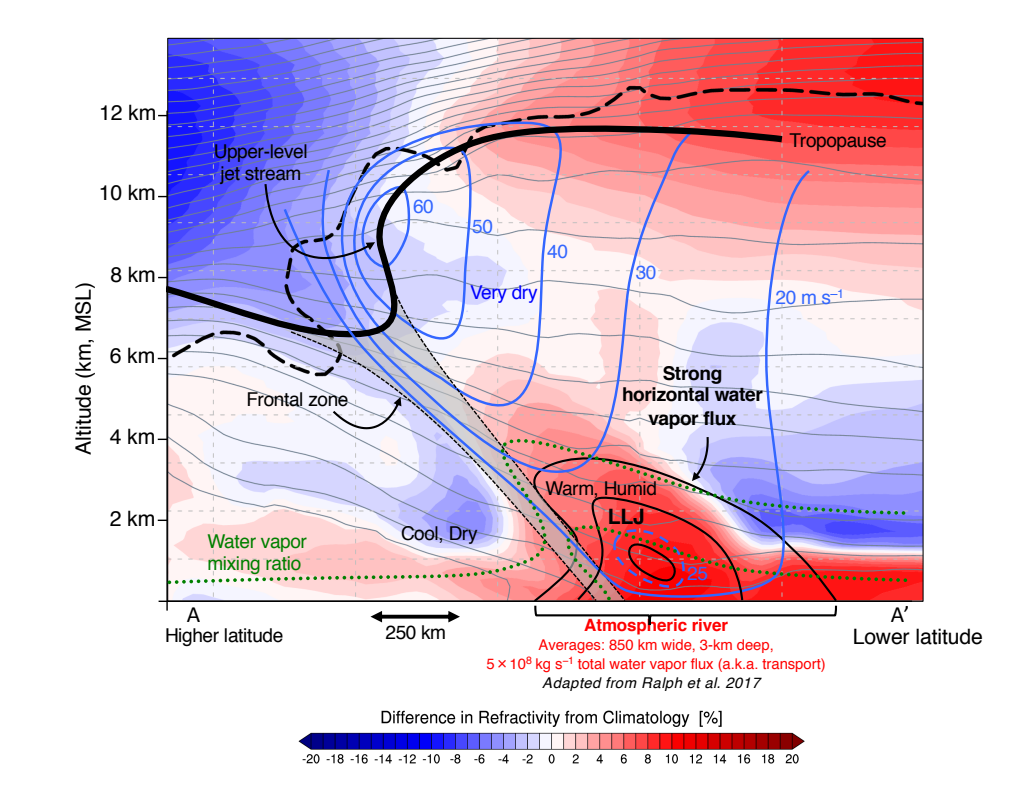
20 ARs hitting the U.S. west coast within three months

AR forecasts have large errors.



Large forecast errors in the area where AR is present

AR structure can be seen in refractivity.

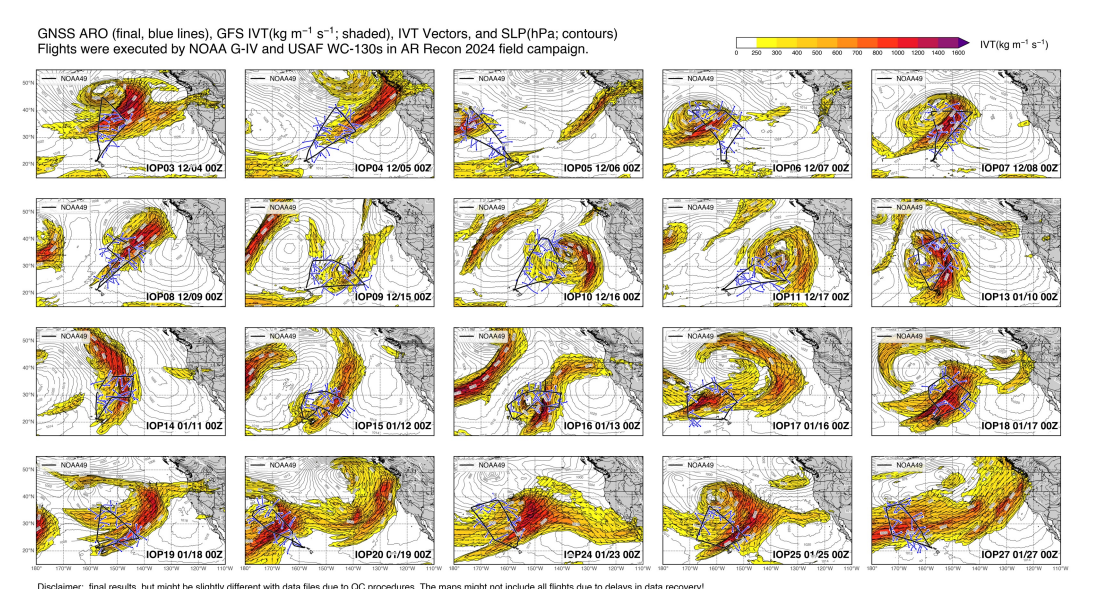


- ARO observations supplement dropsondes without additional expendable costs and provide a link to the larger scale environment.
- The AR structure (concentrated moisture) can be identified in the refractivity and reflective bending, as reflected in water vapor pressure.
- The assimilation of ARO data into numerical models shows positive impacts and corrects the moisture, temperature, and wind fields.

ARO can contribute to AR forecasting.

3. ARO in AR Recon Campaign

ARO is deployed on NOAA and USAF aircraft.



A total of 20 flights were executed by NOAA G-IV during AR Recon 2024.

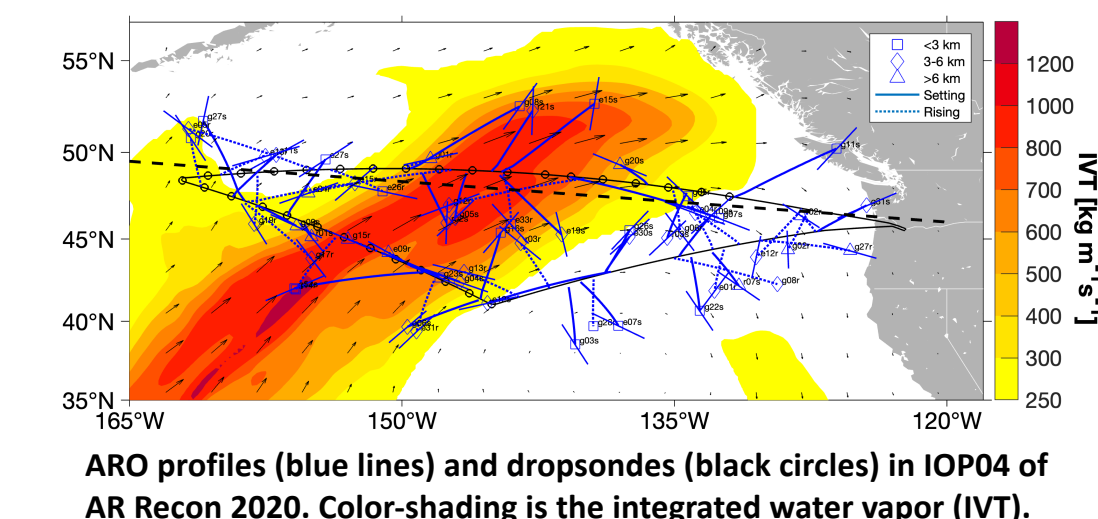
- The Airborne Radio Occultation (ARO) instrument has been deployed on NOAA G-IV jets since 2018 and USAF WC-130s since 2023. **This study presents results solely from NOAA G-IV.**
- Commercial off-the-shelf geodetic (closed-loop) GNSS receivers and raw GNSS signal (open-loop) recorders are both deployed onboard the aircraft, using full-GNSS antennas on the aircraft fuselage. **This study presents results from close-loop geodetic GNSS receivers.**
- The ARO receivers track the major GNSS signals (GPS, GLONASS, Galileo, and BeiDou – still under evaluation).



ARO is a key component in the AR Recon.

- The AR Reconnaissance (AR Recon) campaign collects upstream offshore observations to improve initial conditions in NWP models.
- The flight tracks are planned to target AR key features and sensitive areas identified using adjoint and ensemble model techniques.
- The campaigns are coordinated among one to several aircraft from NOAA and USAF, and many ground observations, including radar, radiosonde and surface measurements.
- ARO, with its invasive nature, can obtain extra observations in restricted airspace and over land without additional costs.

ARO complements dropsonde and radar.



ARO profiles (blue lines) and dropsondes (black circles) in IOP04 of AR Recon 2020. Color-shading is the integrated water vapor (IWV).

Statistics of ARO in 7 years of AR Recon campaigns between 2018 and 2024.

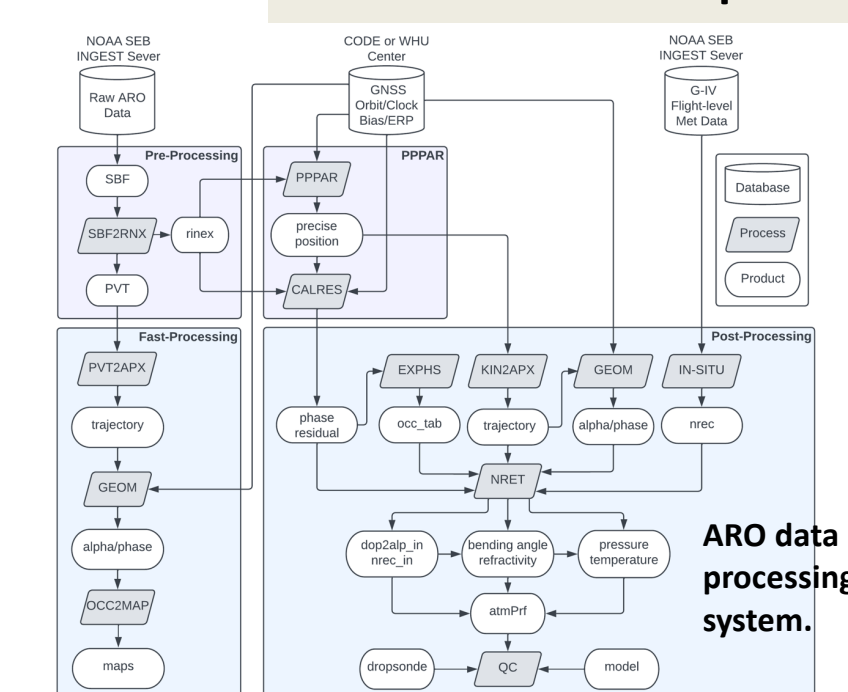
	GPS	GLONASS	Galileo	BeiDou	Rising	Setting	Total
2018	75	39	49	85	85	114	
2019	27	16	19	29	33	62	
2020	335	154	197	325	361	686	
2021	374	255	243	364	508	872	
2022	193	137	123	55	185	323	508
2023	445	323	302	140	525	666	1121
2024	293	240	202	94	314	515	829

A large ARO dataset is available now.

- ARO profiles (blue lines; projected onto mapview) are quasi-randomly but densely distributed along the flight tracks (black line).
- During the recon flights over the northwest Pacific, an average of 6-7 profiles were retrieved per flight hour.
- ARO bending angle and refractivity profiles complement dropsondes and Doppler radar to comprehensively sample the stormy AR environment.
- ARO dataset can be found here: <https://agsweb.ucsd.edu/gnss-aro/>.
- AR Recon can be found here: https://cw3e.ucsd.edu/arrecon_overview/.

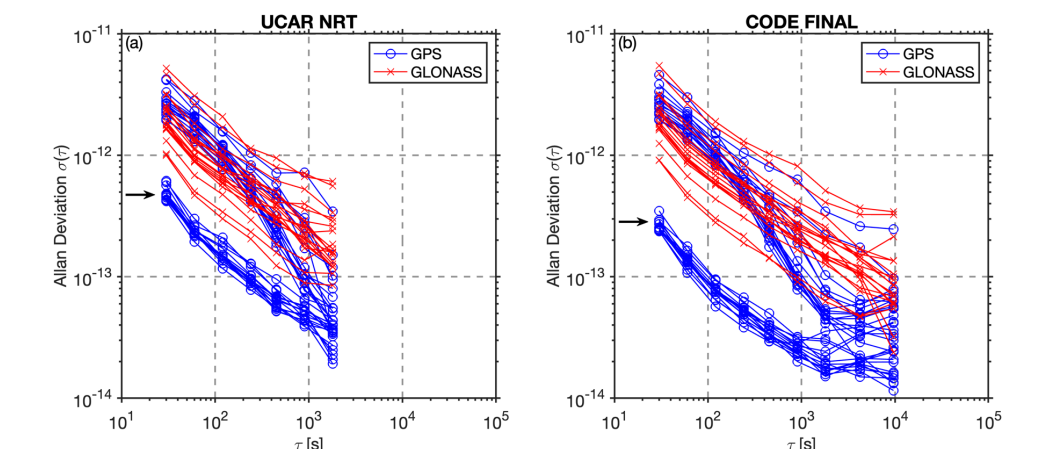
5. Near-Real-Time ARO Operation

An ARO data processing system was established.

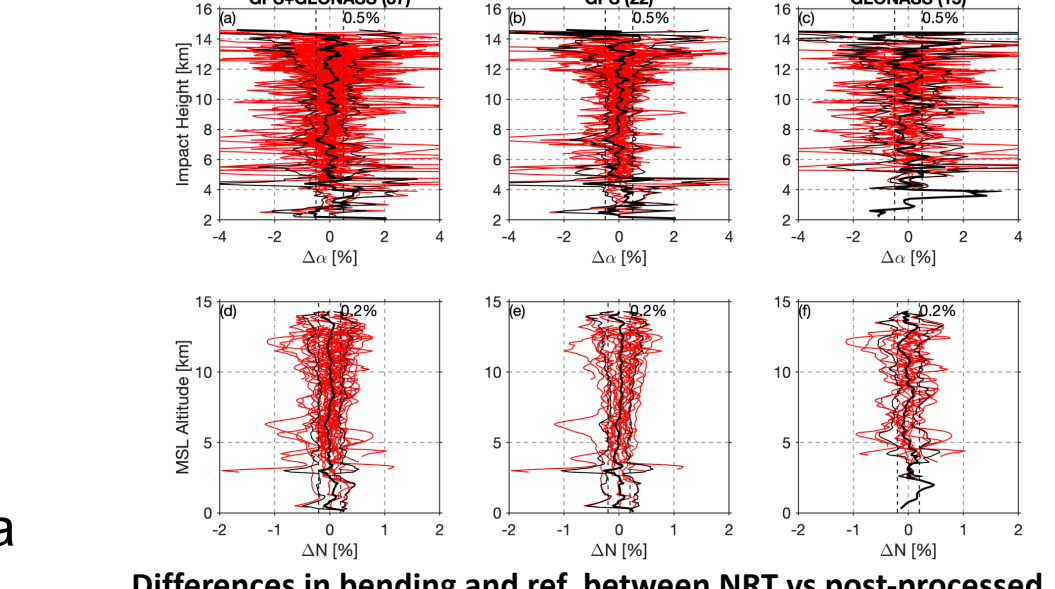


- ARO data processing relies on the availability of GNSS products (orbit, clock, bias, and ERP).
- Raw ARO data was migrated into the G-IV real-time SATCOM data stream and transferred to the NOAA ground server during all flights.
- UCAR CDAAC provides one stream of the GNSS satellite clock correction in real time.
- ARO data processing is under development at SIO.
- We aim to deliver the NRT ARO products with a 1-2 hour delay upon data recovery.

- CDAAC real-time GNSS clock correction has a 1-2 ns RMS difference from CODE final products.
- The modified Allan deviation (MDEV) characterizes the stability of the GNSS satellite clock over a certain time.
- MDEVs better (less) than 10⁻¹² are achieved for most satellites for a time longer than 100 sec.



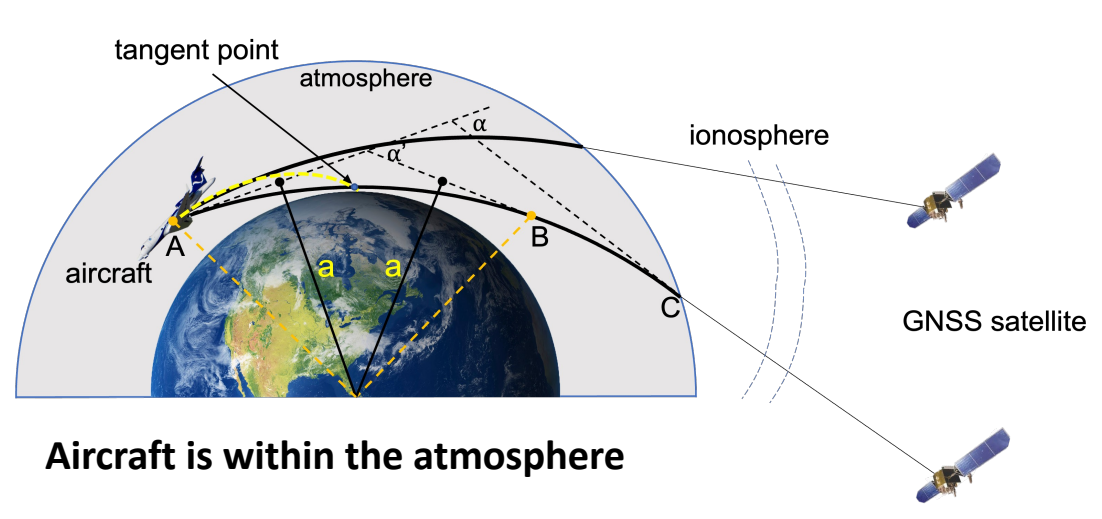
- An offline test showcases that the differences in the bending angle and refractivity, between the NRT and post-processed results, are about 0.5% and 0.2%.
- Final (atmPrf and BUFR) products will be released online and transferred via FTP to the GTS server.



Near real-time ARO processing is under development.

2. Airborne Radio Occultation (ARO)

ARO has high vertical resolution.



ARO has a special asymmetric geometry.

- Compared to spaceborne RO, such as COSMIC, the ARO geometry is NOT symmetric relative to the tangent point as the aircraft is flying within the neutral atmosphere.
- The ARO instrument receives GNSS signals traveling nearly horizontally through the atmosphere, which sample the atmospheric refractivity profile with high vertical resolution.

$$N = (n - 1) \times 10^6 = 77.6 \frac{P}{T} + 37.3 \times 10^6 \frac{P_w}{T^2}$$

- The ARO instrument receives GNSS signals traveling nearly horizontally through the atmosphere, which sample the atmospheric refractivity profile with high vertical resolution.
- The refractive bending angle is integrated along the ray path from the receiver to the tangent point altitude, then to the GNSS satellite. The asymmetric geometry requires additional corrections for the in-situ refractivity and the refractivity above the receiver.

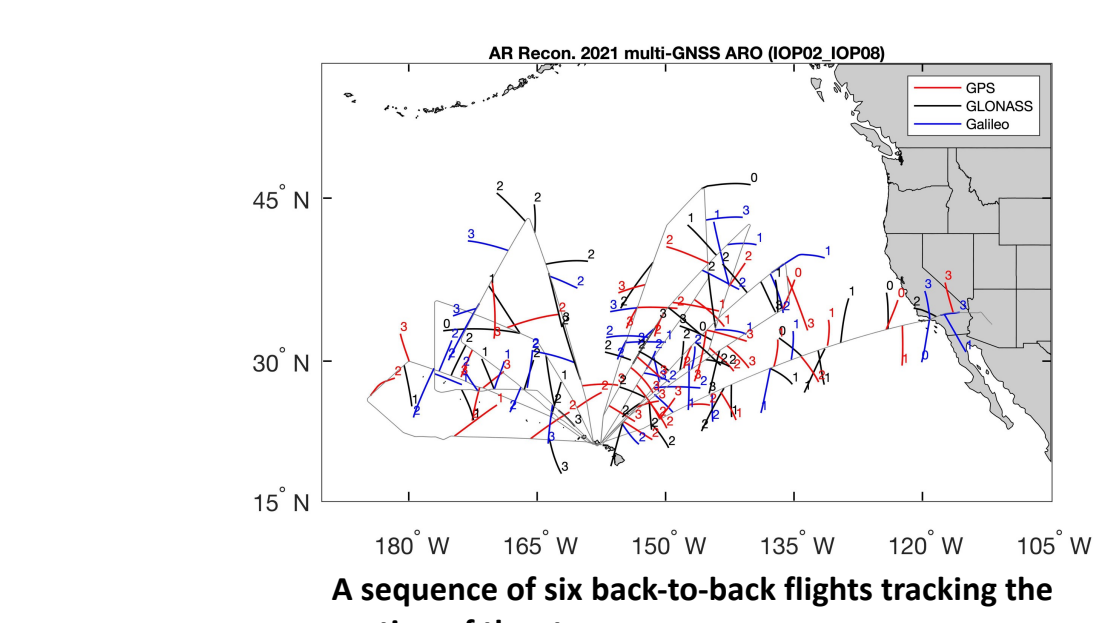
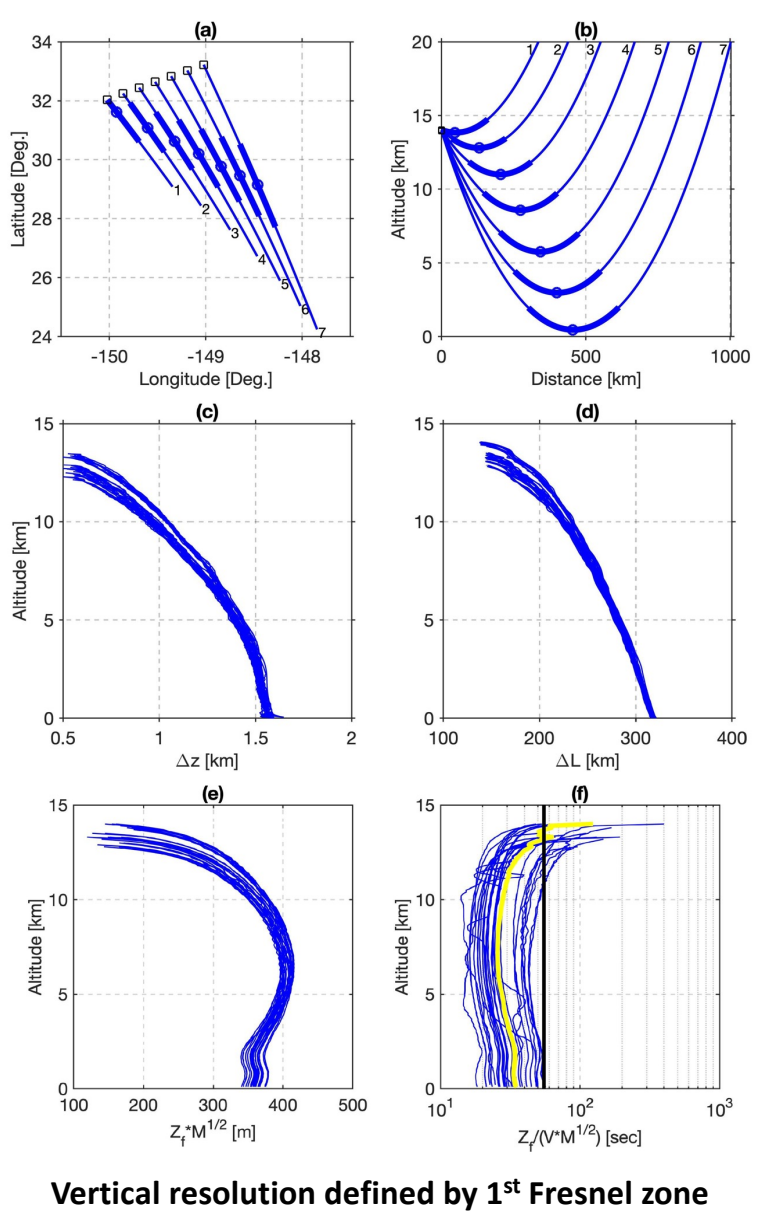
$$\alpha(a) = -2a \int_{r_r}^{r_s} \frac{1}{n} \frac{dn}{dr} \frac{dr}{\sqrt{n^2 r^2 - a^2}} - a \int_{r_r}^{r_s} \frac{1}{n} \frac{dn}{dr} \frac{dr}{\sqrt{n^2 r^2 - a^2}}$$

- The partial bending angle corresponds to the accumulated bending from the symmetric segment of the ray path below the altitude of the receiver. The partial bending angle (difference between positive and negative elevation angle bending) is inverted using the Abel transform to retrieve the refractive index.

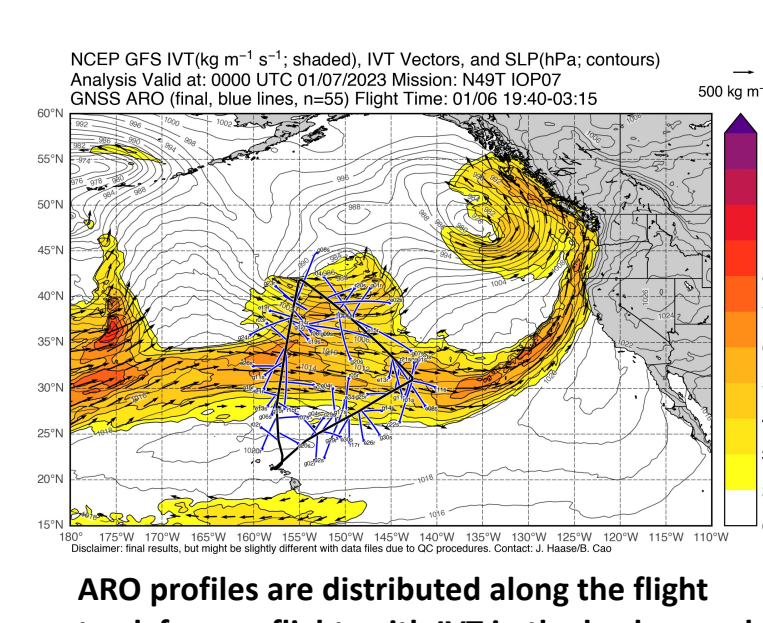
$$n(a) = n_R \cdot \exp\left(\frac{1}{\pi} \int_a^{r_s} \frac{\alpha'(x) dx}{\sqrt{x^2 - a^2}}\right)$$

- The partial bending angle corresponds to the accumulated bending from the symmetric segment of the ray path below the altitude of the receiver. The partial bending angle (difference between positive and negative elevation angle bending) is inverted using the Abel transform to retrieve the refractive index.

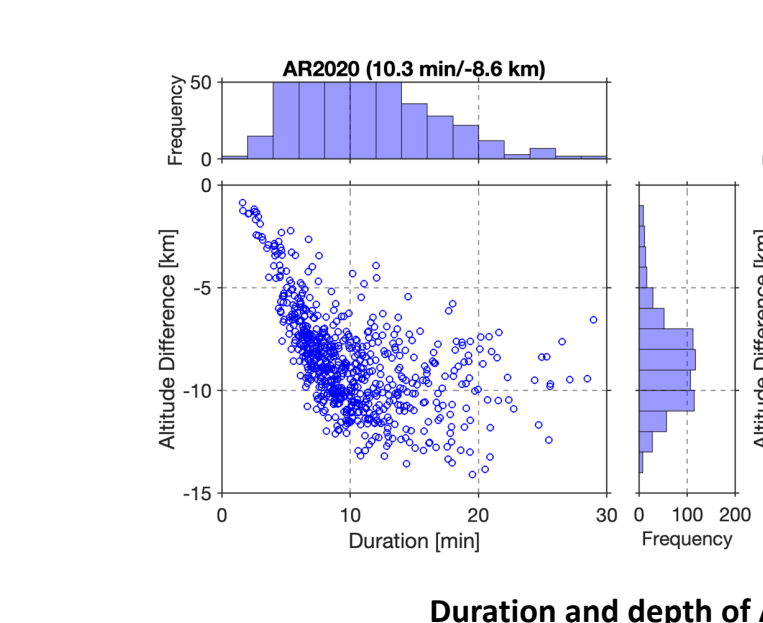
$$Z_F = 2\sqrt{\frac{\lambda L_T L_R}{L_T + L_R}}$$



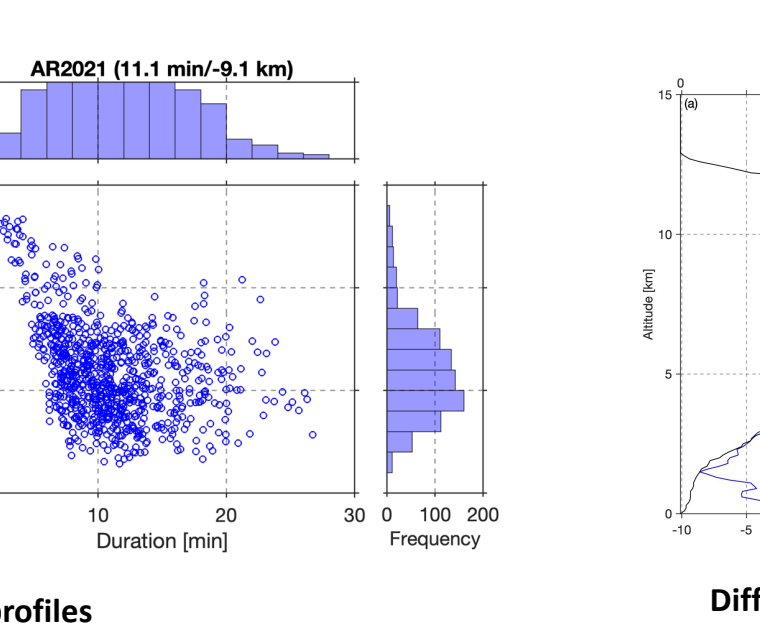
A sequence of six back-to-back flights tracking the motion of the storm.



ARO profiles are distributed along the flight track for one flight, with IWV in the background.



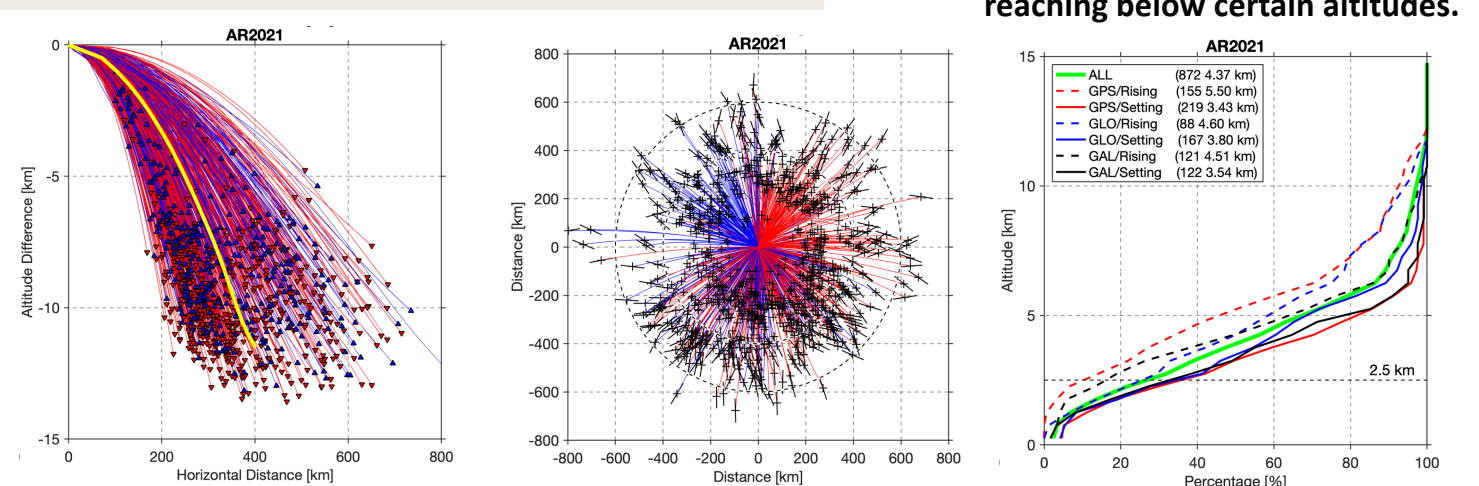
Duration and depth of ARO profiles



Difference in the refractivity between ARO and closest dropsonde

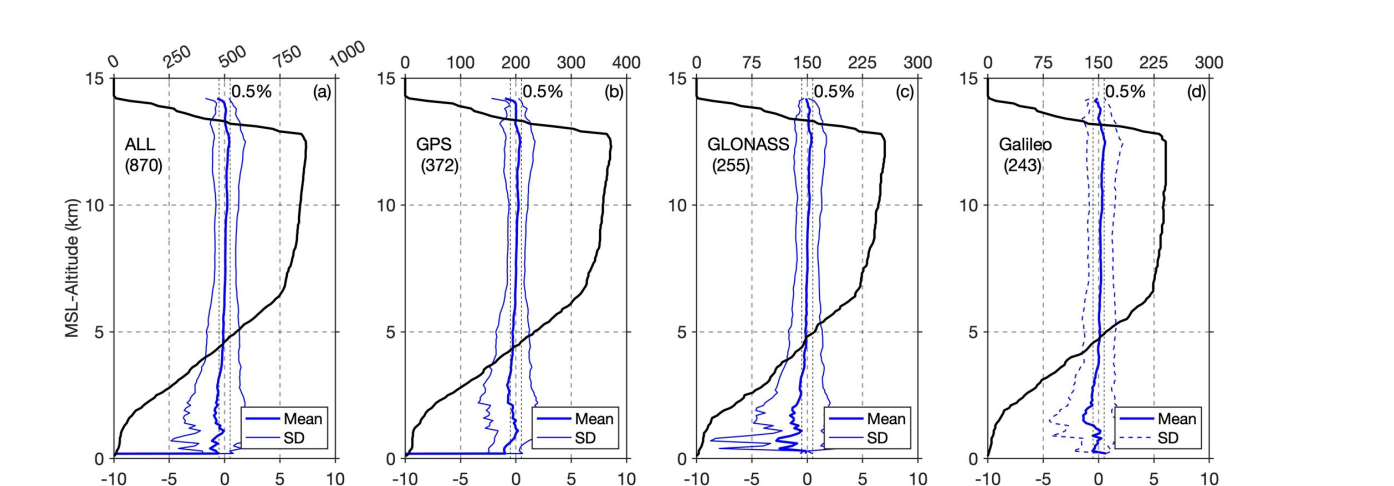
4. ARO Sampling Characteristics and Accuracy

ARO profiles are slanted.



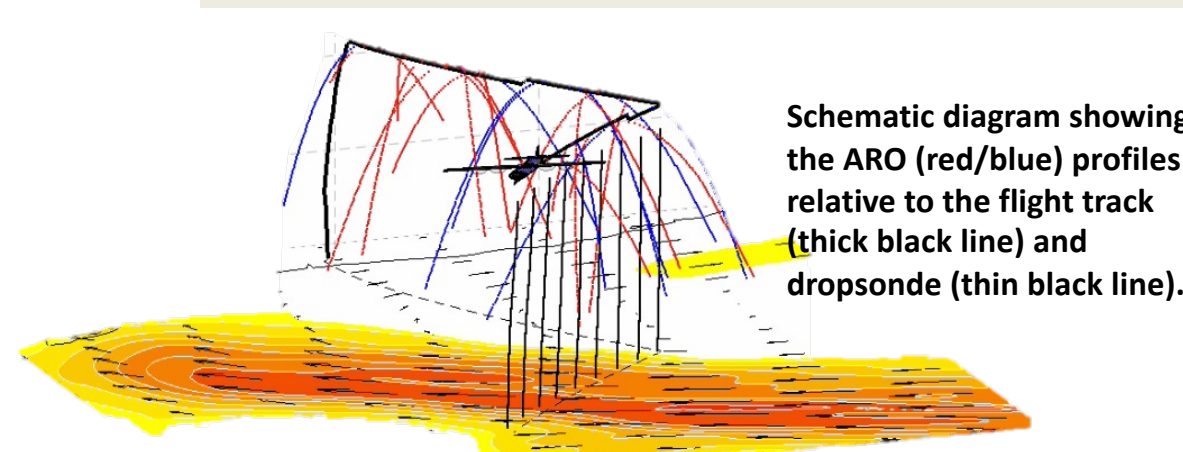
- The average horizontal drift distance is about 400 km when tangent points are about 10 km below the aircraft's cruise altitude, but it can be as far as 600 km.
- The drift orientation occurs in a few principal orientations determined by the orbital planes of the rising (red) and setting (blue) GNSS satellites.
- Most profiles truncate at about ~4 km altitude when the receivers lose track of the GNSS signal in closed-loop mode.
- Setting occultations generally penetrate about 1 km deeper than rising ones.

ARO refractivity is within a 0.5% bias with ERA5.



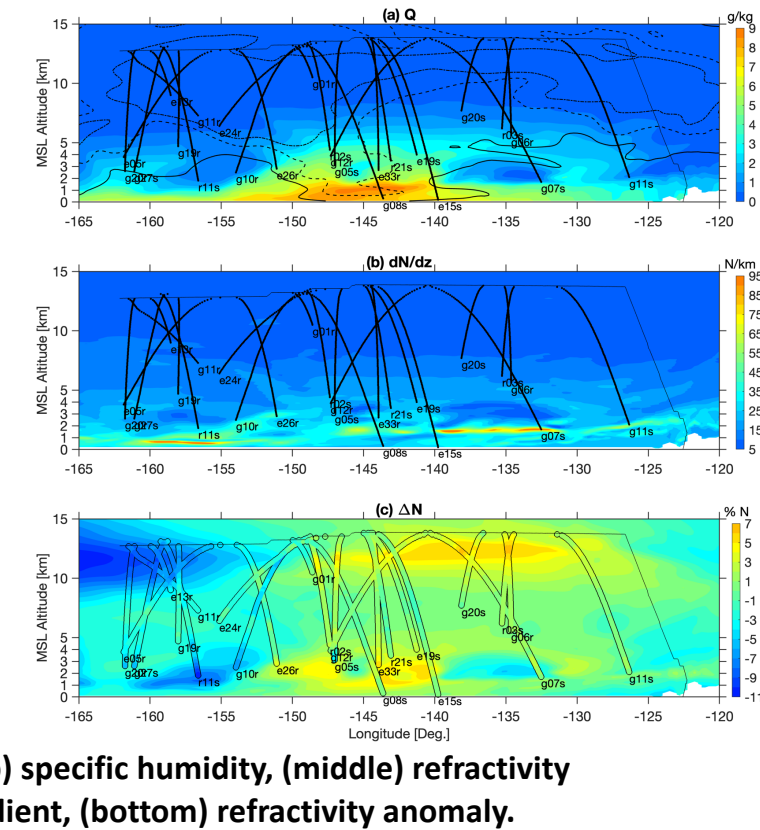
- The refractivity of ERA-5 is interpolated to the locations of the drifting ARO tangent points.
- Above 5 km, the difference between ARO and the ERA-5 model is 0.5% mean and 2% standard deviation (SD). The SD increases to 3% below 5 km.
- There is no apparent difference among the occultations of different constellations.

ARO provides a 3-D sampling.



- The ARO profiles are closely aligned with the aircraft location, so the target sensing area can be planned.
- Slanted profiles extend the probing range from underneath the flight track to sideways and provide a unique 3D sampling.

ARO resolves AR synoptic environment.



- A vertical transect was created from the ERA-5 reanalysis that crosses the AR along the northern flight segment.
- Most ARO profiles terminate above the sharp gradient (dN/dz > 50 N/km) due to the abundance of moisture.
- The ARO observed refractivity closely matches the ERA-5 and resolves the structure above and around the AR core.
- Work based on open-loop tracking is underway to extend the profiles to the surface.

6. Summary

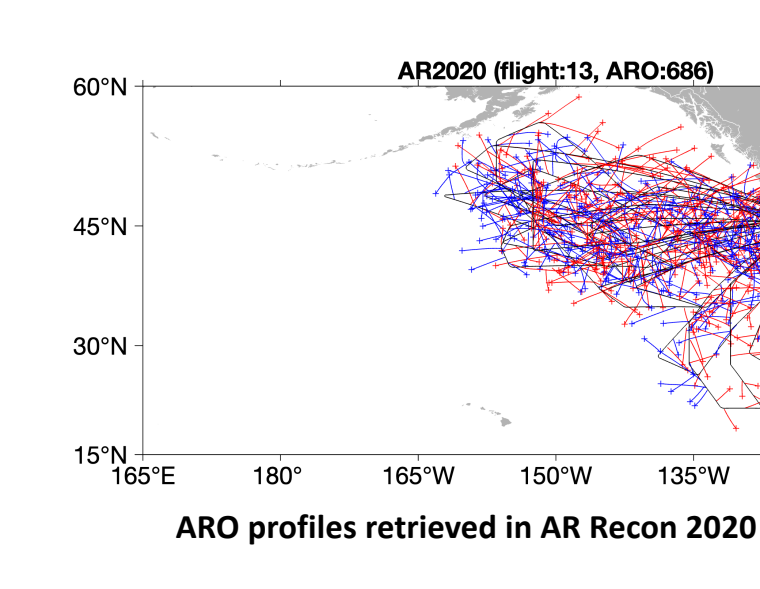
- The ARO has successfully run on multiple NOAA and USAF aircraft and delivered valuable mid-troposphere observations for AR research and forecasting.
- With its unique slant profiling feature, ARO complements the dropsonde and augments the aircraft sensing area sideways from flight tracks.
- Good ARO data quality is demonstrated by a difference of 0.5% mean and 2% SD (above 5 km) when compared with ERA-5.
- A large multi-year (and growing) ARO dataset is available now (<https://agsweb.ucsd.edu/gnss-aro/>).
- Near-real-time ARO operation is currently under development, and we are working with NCEP on the data format and transmission to GTS.
- ARO is planned to be deployed on more aircraft, including NASA ER-2, DLR HALO, and NASA NATURE (B-777).

References

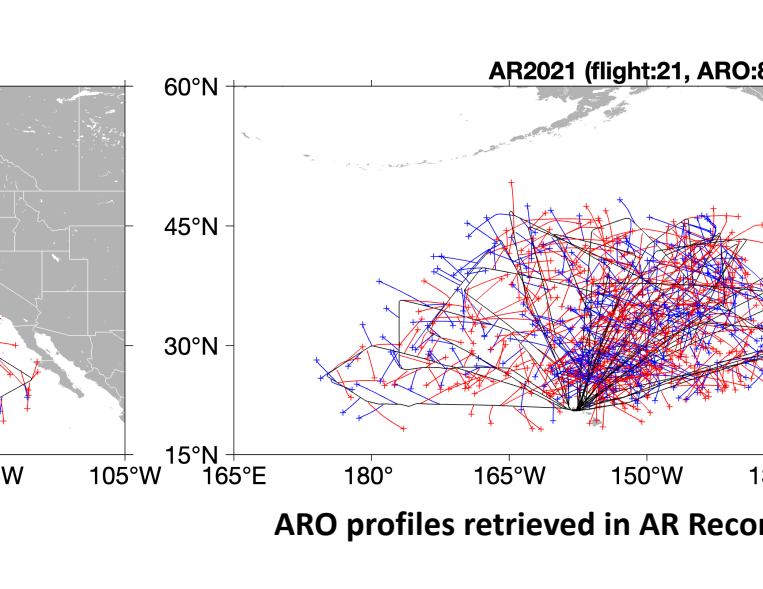
Ralph et al., 2020, 2021, BAMS, Haase et al., 2021, JGR-A, Cao et al., 2022, ACP, Hordyniec et al., 2024, JAMES, Cao et al., 2024, AMT.

Acknowledgments

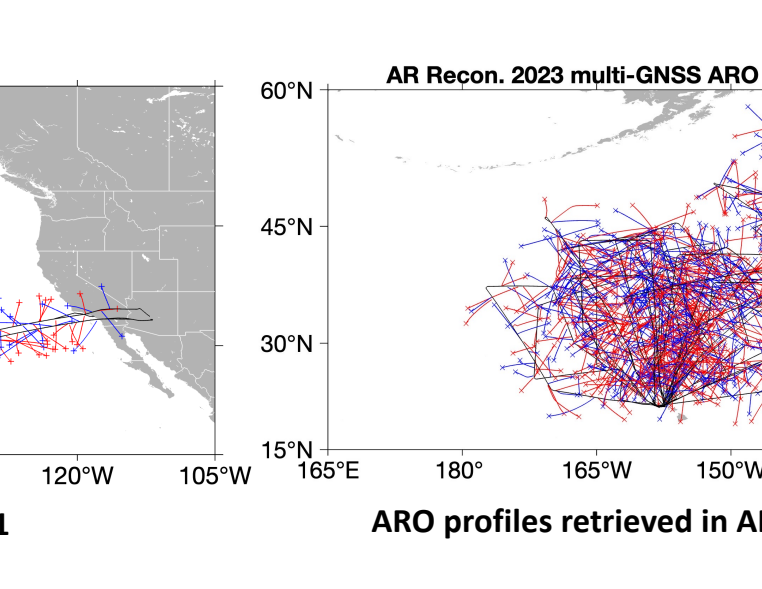
This work was supported by NSF Grants AGS-1642650, AGS-1454125, AGS-2402728, and NASA Grant NNX15AU19G. Support was also provided through the UCSD Center For Western Weather and Water Extremes (CW3E) Atmospheric River Research Program from the California Department of Water Resources and from the US Army Corps of Engineers. The authors sincerely acknowledge the continued support from NOAA Aircraft Operation Center, in particular, G. Defeo, J. Parrish, A. Lundry, and L. Miller for assisting with installation and operation of the ARO equipment on the G-IV aircraft and implementing the SATCOM transfer of the ARO data. UCAR/CDAAC is acknowledged for sharing their real-time GNSS clock corrections.



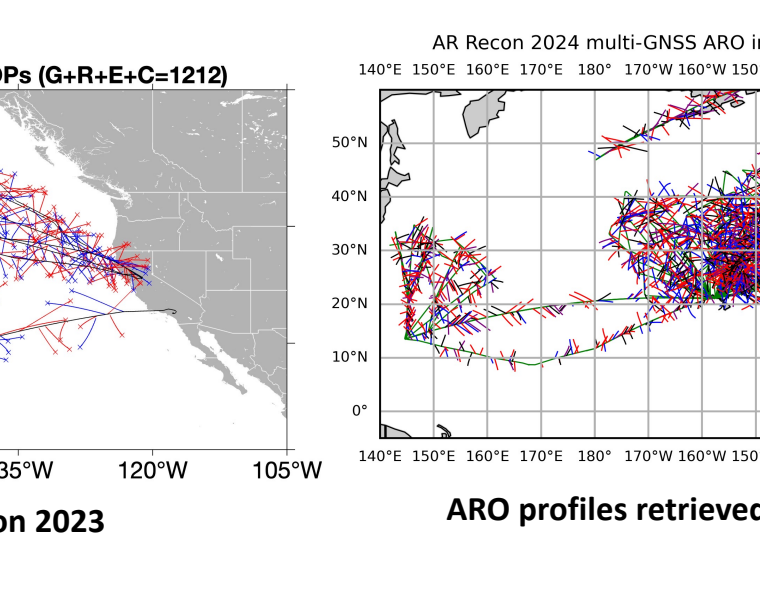
ARO profiles retrieved in AR Recon 2020



ARO profiles retrieved in AR Recon 2021



ARO profiles retrieved in AR Recon 2023



ARO profiles retrieved in AR Recon 2024